HEAT TRANSFER LIMITATION DURING RAPID DEPRESSURIZATION

J.C. Luxat and D.R.Novog
Department of Engineering Physics
McMaster University

Abstract

During depressurization events, such as large break LOCA, there is a large increase in the rate of vapour bubble nucleation on heated surfaces of fuel elements arising from the transient increase in wall superheat of the fuel sheaths. Continued nucleate boiling and associated high rates of vapour generation are dependent upon the balance between liquid resupply and vapour nucleation and transport away from heated surfaces. These competing processes are analyzed. Results demonstrate that during initial blowdown the boiling contribution to coolant voiding is limited by vapor nucleation and transport and not necessarily by onset of critical heat flux.

1. Introduction

The early depressurization (blowdown) of pressurized, hot water coolant in a reactor heat transport sytstem is characterized by rapid decompression during which local pressure rapidly decreases to the local saturation pressure of the fluid. If the rate of depressurization is very high, as might be expected in a large break Loss of Coolant Accident (LOCA), with the heat transport system coolant initially subcooled, then the pressure may transiently undershoot the local fluid saturation pressure until sufficient vapour generation occurs causing a pressure recovery to saturation pressure. Vapour generation, and the accompanying large change in specific volume associated with liquid to vapour phase change, reduces the subsequent depressurization rate to lower values typical of two-phase blowdown.

The heat transfer rate from the heated fuel sheath surface of elements in fuel bundles during the early blowdown period will be strongly dependent upon the rate of vapour generation as well as the distribution and transport of vapour in the liquid coolant phase within the bundle. The physical basis of vapour nucleation processes, the transport of vapour within the fuel budle and empirical evidence relevant to heat transfer during transient depressurization are discussed below. It is shown that, for the time scale of early blowdown in CANDU heat transport systems, vapour nucleation and transport processes impose limitations on heat transfer from fuel elements, particularly in events in which the coolant flow in fuel channels decreases significantly.

2. Flow Boiling

Under steady flow and pressure conditions, typical of those expected under normal plant operation, heat transfer from fuel element sheaths to the coolant is governed by turbulent convection processes. The fuel sheath temperatures are higher than the local average bulk temperature of the coolant away from the heated surfaces of the sheaths. A temperature

gradient exists in the thermal boundary layer of fluid directly adjacent to the heated surface. Diffusion of the hotter fluid in this boundary layer into the cooler bulk fluid is assisted by turbulent mixing, with the degree of mixing being the dominant factor in moving hotter fluid away from the surface and bringing colder fluid into the boundary layer. When boiling occurs, vapour bubbles develop at nucleation sites on the heated outer surface of fuel elements and grow until they reach a critical size and detach from the surface. If the bulk fluid away from the surface liquid film layer is subcooled, then the vapour bubbles condense in the fluid (typical of subcooled boiling behaviour), whereas if the bulk fluid is saturated the departing vapour bubbles remain dispersed in the liquid (bubbly flow) or interact and coalesce with other vapour bubbles to form larger vapour bubbles and vapour structures typical of two-phase flow regimes (*e.g.*, churn-turbulent, plug and slug flow).

A governing factor in the vapour nucleation processes associated with the nucleate boiling heat transfer mode is the replenishment of the liquid phase at active nucleation sites following the nucleation, growth and detachment of a vapour bubble. If liquid replenishment cannot occur at rate to balance the vapour production at nucleation sites, then the heated surface will dry out and a vapour film blanketing a region of the surface - a "drypatch" - will develop, with heat being transferred by conduction through the vapour film (film boiling). If the drypatch expands to cover the majority of the heated surface then film boiling will become the dominant mode of heat transfer, with a resultant substantial increase in the temperature of the surface.

Under conditions of rapid depressurization the balance between vapour generation at active nucleation sites and the replenishment of the liquid film layer to refill the sites will be strongly influenced by the transient nucleation rate, bubble growth, detachment and coalescence of bubbles, together with the subsequent transport of bubbles away from the heated surface. Therefore, it is necessary to consider the dynamics of vapour generation and transport in additional detail. If the rate of vapour formation is sufficiently high, then vapour transport away from the fuel sheath may become a factor limiting the rate at which liquid replenishment occurs, thereby limiting the efficiency of nucleate boiling heat transfer even though drypatch formation has not yet occurred. This paper discusses the limitations on nucleate boiling heat transfer associated with these factors.

3. The Dynamics Of Vapour Generation

The physics of bubble nucleation, proposed by Bankoff [1], has been further developed and analyzed by Hsu [2] and Han and Griffiths [3]. These conceptual models, generally referred to as classical nucleation theory, involve a repetitive process of bubble nucleation at surface cavities, bubble growth and detachment, followed by a waiting period before the next nucleating bubble forms. The waiting period is influenced by the subcooling of the liquid that replenishes the nucleation site and by the superheat of the wall relative to the coolant. The number of nucleation sites per unit area of the heated surface, the nucleation site density, n/A, is controlled predominantly by the wall superheat temperature and can be represented by the following empirical relationship [4-6]:

$$\frac{n}{A} = C\left(\frac{1}{r_c}\right)^m \qquad [\text{cm}^{-2}] \qquad (1)$$

where:

r_c is the critical cavity radius
C, m are constants

The critical cavity radius is a function of wall superheat and fluid interfacial properties. In situations where the liquid phase density is significantly greater than the vapour phase density, as would be the case for nuclear reactor heavy water or light water coolants, the critical cavity radius is given by:

$$r_c = \frac{2\sigma T_{sat}}{\rho_v h_{fg} \Delta T_{super}}$$

$$\Delta T_{super} = T_w - T_{sat} \qquad (2)$$

where:

T_{sat} is the fluid saturation temperature [K]
T_w is the wall temperature [K]
ΔT_{super} is the wall superheat temperature [K]
σ is the liquid phase surface tension at the liquid -vapour interface
ρ_v is the vapour density [kg/m^3], and
h_{fg} is the latent heat of vaporization [kJ/kg]

Substituting eq. (2) into eq. (1) yields an expression for the nucleation site density as:

$$\frac{n}{A} = C\left(\frac{\rho_v h_{fg} \Delta T_{super}}{2\sigma T_{sat}}\right)^m \qquad (3)$$

Typical values of C and m from the literature [8] are in the range $1\text{x}10^6$ to $6\text{x}10^6$ and 4.5 to 5.4, respectively, with n/A in units of cm^{-2}. Some experimenters have found a dependency of the correlating coefficients in the characteristic dimensions of the nucleation cavities. The coefficients used here are typical values obtained from the literature [7,8], namely C= $5.8\text{x}10^6$ and m= 4.5.

Equation (3) is plotted as a function of wall superheat for pressures between 9.5 and 8.0 MPa, which are typical pressures in the fuel channels during the early stages of a critical break large LOCA in a CANDU reactor (Figure 1). This plot shows the rapid increase in nucleation site density with increasing wall superheat and the decrease in nucleation site density with pressure for a constant wall superheat. The increase in nucleation site density with wall superheat, and hence the increased heat transfer from the wall due to vaporization,

reflects the well established saturated nucleate boiling behaviour in which heat flux increases with wall superheat (the boiling curve). Additionally, it has also been observed that nucleation site density, with other parameters fixed, increases approximately with heat flux squared [8], i.e.,

$$\frac{n}{A} \propto q^2 \qquad (4)$$

where:

q is the average surface heat flux

3.1 Inferred Nucleation Site Density

The approximate magnitude of nucleation site density at the onset of dryout in a 37-element fuel bundle can be inferred from steady state CHF data and correlations of the data. This has been evaluated using values of dryout heat flux at different mass flow rates calculated for a constant quality of 5% at a pressure of 9 MPa with the flux-corrected local conditions correlation developed from full-scale water CHF tests. Pre-dryout nucleate boiling heat transfer coefficients are assumed to vary with mass flow rate (or mass flux, G) according to $G^{0.8}$ and are used to calculate the wall superheat, ΔT_{super}, for nucleate boiling at the incipient dryout heat flux. This wall superheat is used, in turn, to calculate the corresponding nucleation site density according to equation (3). The results are shown in Table 1, including extrapolated values at flow rates lower than the range of the CHF test data. Interestingly, the critical values of wall superheat and nucleation site density vary in a narrow range for the fixed fluid pressure and quality conditions assumed, as one would expect from the flow boiling curve.

This could be interpreted as indicating the appropriateness of the extrapolation of the CHF correlation to very low flows. However, the validity of the extrapolation is based on the assumption that vapour distribution within the fuel bundles does not change significantly in going from the flows at which the data has been collected to lower flows. This is an incorrect assumption when flow decreases to values where bubble rise and vapour transport due to boiling become significant (i.e., mass flow rates less than 2 kg/s). It is expected that the CHF correlation will be a conservative upper bound on boiling heat transfer as flows become very low, as discussed below.

Vapour nucleation site density alone does not provide a sufficient description of the processes controlling boiling heat transfer. Equally important are the transport processes governing the movement of vapour bubbles away from the nucleating sites and the replenishment of liquid at these sites. This is discussed below.

3.2 Vapour Transport From Heated Surface

Vapour bubble growth occurs at the nucleation sites until the bubbles attain a size at which they detach from the wall surface and are free to move into the bulk of the fluid. At this

time, liquid from the liquid micro-layer region adjacent to the wall can be transported to refill the cavities, which in turn, results in cooler liquid being mixed into the film region. Following a waiting period, during which the liquid in the micro-layer is heated up to saturation and then becomes superheated due to proximity to the wall, the process of nucleation at the cavities, bubble growth and detachment repeats. This waiting period has some dependency on the subcooling of the bulk liquid [10].

If the density of nucleating sites and the rate of vapour generation becomes high, then bubble coalescence can occur. As a consequence of bubble coalescence, the replenishment of the liquid to the micro-layer can be impeded, resulting in the formation of a local drypatch region on the heated wall. The extent of the drypatch will be a function of the availability and distribution of liquid in the region of the drypatch, the intensity of local liquid mixing accompanying bubble detachment, the rate of liquid mass and energy transport toward the wall and the rate of vapour generation. As the extent of the drypatch increases, the overall heat transfer from the wall will decrease and film boiling heat transfer becomes increasingly dominant – analogous to a "drypatch spreading" phenomenon.

Vapour phase transport away from the nucleating sites will, for a horizontally oriented heated surface such as a fuel element sheath, have a three-dimensional velocity field. The three components of the vapour velocity are:

a) the "boiling" velocity, v_B, associated with bubble detachment, which is in a direction perpendicular to the heater surface;

b) the bubble rise velocity, v_{Br}, which is in a vertical direction and is due to buoyancy effects associated with density differences in the gravitational field; and

c) the bubble entrainment velocity, v_{Be}, which is axially oriented and is due to interfacial drag forces associated with the relative velocity between the axially convected liquid phase and the vapour bubbles.

The magnitude of these three components will vary, depending upon heat flux, local fluid conditions and the liquid phase flow rates in the fuel bundle, and will determine the extent to which vapour transport from the heated surface is controlled by forced convection or local (natural) convection. The relative importance of these three velocity components under two-phase boiling conditions can be quantified by considering the characteristic dimensions and transport times associated with vapour transport in the three dimensions - in this instance these are the characteristic dimensions within a fuel bundle. This is discussed below.

3.2.1 Boiling Velocity

The boiling velocity represents an average velocity associated with vapour generated at the heated surface moving away from the wall, and is given by:

$$v_B = \frac{q}{\rho_v h_{fg}} \tag{5}$$

Where: q is the average surface heat flux [kW/m^2]

The characteristic dimension for vapour transport radially outward from the fuel sheath, λ_B, ranges from the gap between two adjacent elements (0.0018 m), the minimum value, and the equivalent hydraulic radius (half the equivalent hydraulic diameter) of subchannels (0.00455 m). The characteristic transport time associated with the boiling velocity for fuel elements is:

$$\tau_B = \frac{\lambda_B}{v_B} \tag{6}$$

The physical interpretation of this transport time is that it is the average time taken for a vapour bubble generated from the surface of one fuel element to move a distance such that it cannot be distinguished from a vapour bubble generated at the same time from the surface of a neighbouring element.

3.2.2 Bubble Rise Velocity

The vertically oriented bubble rise velocity for a bubble freely moving in a stagnant liquid fluid is given by the Zuber-Findlay expression for drift flux in bubbly flow (Reference 10):

$$v_{Br} = 1.41\left[\frac{g\sigma(\rho_l - \rho_v)}{\rho_l^2}\right]^{1/4} \tag{7}$$

The characteristic dimension for vertical bubble rise, λ_{Br}, is in the range of the fuel element radius plus the inter-element gap (0.08 m) to the diameter of a fuel element plus the inter-element gap (0.015 m), and the characteristic transport time for bubble rise is:

$$\tau_{Br} = \frac{\lambda_{Br}}{v_{Br}} \tag{8}$$

The bubble rise characteristic transport time can be interpreted as the time for a bubble detaching from a fuel element sheath to move a sufficient vertical distance such that it can interact and coalesce with vapour bubbles generated from an element at a higher elevation.

3.2.3 Entrainment Velocity

Immediately on detaching from the heated wall surface the expanding vapour bubbles will have negligible axial velocity and will subsequently be accelerated by the interfacial drag force between the vapour bubble and the axially flowing liquid. This drag force acts to entrain the bubbles into the moving liquid. Assuming a negligible time to accelerate the

bubble, the axial vapour entrainment velocity, v_{Be}, will, in the limit, approach the velocity of the liquid phase given by:

$$v_{Be} = \frac{W_l(1-\chi)}{\rho_v A_{flow}} \tag{9}$$

where:

- W_l is the cross-sectional average liquid mass flow rate at the location in the channel
- A_{flow} is the cross-sectional flow area of fuel bundle in the channel
- χ is the local fluid mass quality

The characteristic dimension associated with bubble entrainment in axial flow parallel to the surface of a fuel element, λ_{Be}, is of the order of half the length of a fuel bundle (0.25 m). The corresponding characteristic transport time is:

$$\tau_{Be} = \frac{\lambda_{Be}}{v_{Be}} \tag{10}$$

This characteristic transport time represents the average time taken to transport vapour generated from fuel elements within a bundle to a neighbouring bundle where the vapour can interact and coalesce with vapour being generated in the neighbouring bundle.

As developed above, the characteristic transport time represents the time required to transport vapour from a particular fuel element in the three geometric dimensions a sufficient distance such that the dispersed vapor volumes can interact and coalesce (and hence influence the local vapour content) with vapour being generated and transported in the same direction from neighbouring heated surfaces. Typical vapour velocities, characteristic dimensions and transport times in a CANDU 37-element fuel bundle are given in Table 2 for heavy water at 9.0 MPa. The ranges of heat fluxes and liquid axial flow rates given in the table are typical of those experienced in the early stages of blowdown in a large break LOCA.The data from Table 2 is plotted in Figure 2 as a function of liquid coolant mass flow rate.

As graphically demonstrated in Figure 2, at liquid flow rates less than approximately 1 kg/s, the characteristic transport times for boiling and vertical bubble rise become significantly less than for axial vapour entrainment. This indicates that, at these flows and lower, both vapour accumulation and phase separation effects will be governed primarily by vapour generation at neighbouring fuel elements within a given bundle, *i.e.*, the effects of axial transport of vapour from one bundle to the next will be significantly delayed and, therefore, will have reduced influence on the heat transfer in a given bundle. Under these conditions, which correspond to those found during the early stages of a critical break LOCA, the heat transfer in the central high powered bundles, which are also in the region of high neutron flux importance, will be strongly limited by the local vapour generation. Therefore, in

addition to the effects of increased nucleation site density and increasing wall superheat, discussed in the previous section, the vapour transport considerations indicate that high nucleate boiling heat flux cannot be sustained. The expected heat transfer conditions are one in which transient CHF will be lower than the value inferred from steady state data at corresponding local fluid conditions. Of equal importance is the fact that coolant voiding due to boiling will tend to be limited by the local transport of vapour, especially in the high power and high neutron importance regions of the core.

4. Behaviour During Large Break LOCA

Large break LOCA events are characterized by a rapid decompression transient in the heat transport system, including the fuel channels. As coolant discharges from the system, the local saturation temperature decreases with decreasing pressure, resulting in void generation due to flashing. In the early stages of the blowdown, rapid vapour nucleation will occur on the fuel element sheaths due to rapidly developing liquid superheat in the micro-layer adjacent to the fuel sheaths. The fuel sheath temperature cannot instantaneously follow the reduction in the bulk coolant saturation temperature associated with the depressurization, and therefore the wall superheat will tend to increase, promoting a rapid increase in bubble nucleation site density on the fuel element sheath surfaces.

The rapid increase in the wall superheat on high powered fuel bundles in the central region of a fuel channel associated with the decrease of the coolant saturation temperature is shown in Figure 3 for the first few hundred milliseconds of a large 100 percent RIH break. As might be expected, this results in a large increase in the nucleation site density, as illustrated by the loci of nucleation site density versus wall superheat, also shown in Figure 3. Relative to the limiting values of nucleation site density inferred from steady state 37-element CHF test data, discussed previously and presented in Table 1, the ability to sustain high nucleate boiling would by impeded early in the transient. This applies in particular to the 100 percent break, where although high reverse flows occur, the coolant enthalpy entering from the reactor outlet header side is high and the wall superheat remains large due to the rapid depressurization.

In a critical break, high nucleation rates will occur initially, but vapour transport considerations become dominant due to the low coolant flows in the channels of the critical pass. In the early stages of blowdown, low flows rapidly develop in the central section of the fuel channel, initially reversing to a low value of approximately -5 kg/s in about 0.2 s and then decreasing to values less than ±1 kg/s by about 0.3 s. Based upon the transport time considerations discussed in the previous section, bubble rise and boiling transport become significant factors influencing the distribution of vapour in fuel bundles at flow rates lower than 2 kg/s. At flow rates below 1 kg/s these vapour transport components will become dominant, as shown in Figure 2. This implies that most of the vapour generated will, in the early stages of blowdown, be in the immediate vicinity of the fuel element sheaths from which the vapour originated and, furthermore, axial liquid transport along the central fuel bundles will occur too slowly to replenish the liquid micro-layer from which vapour is nucleating. Therefore, very early in the blowdown, the vapour nucleation and transport processes will act to limit heat transfer to values lower than those associated with

steady state nucleate boiling.

Experimental evidence from the literature supports the considerations discussed above. For example, transient heat transfer measurements obtained on horizontal heated cylindrical wires, 1.2 mm and 3 mm in diameter, immersed in water in a vessel which was subject to rapid depressurization indicated that (Reference 11):

a) the ratio of transient maximum heat flux to steady state heat flux at the corresponding pressure was less than 1, being in the range of 0.2 to 0.8, and

b) a heated rod with larger heat capacity will make a transition to film boiling more readily upon depressurization. This indicates the effect of increasing wall superheat during the depressurization.

Blowdown experiments in a small scale Freon vessel with a central heater performed to study the occurrence of CHF during blowdown accompanied by a flow reversal (Reference 12) have shown that:

a) early measured CHF is associated with transition from bubbly to annular flows and was independent of the liquid volume in the system,

b) later CHF occurred when the liquid in the test section had significantly depleted, and

c) there is a preferential distribution of liquid to regions away from the heater and the liquid film on the heater could not be replenished as fast as it was being depleted.

5. Analysis of LOCA Heat Transfer

The above experimental observations are supported by consideration of the rapidly increasing bubble nucleation density on the fuel sheath surface during the early stages of blowdown. The fraction of the area of a fuel sheath covered by nucleating bubbles, F_{nb} , is calculated using the following equation:

$$F_{nb} = \frac{A_{nb}}{A_{el}} = \frac{\left(\pi r_b^2 \left(\frac{n}{A}\right)\right)\pi r_b^2}{\pi D_{el} L_{el}} \qquad (11)$$

The numerator of the above equation is the number of nucleation sites under the projected area of a detaching bubble times the projected area of a detaching bubble of radius r_b (i.e. the total projected area of the detaching bubbles). The denominator is the surface area of a fuel element of diameter D_{el} and length $L_{el.}$ The nucleation site density as a function of wall superheat is calculated from equation (3). Using the above area fraction, the fraction of the fuel sheath that is participating in boiling heat transfer, F_b , is obtained from:

$$F_b = 1 - F_{nb} \qquad (12)$$

The boiling heat transfer fraction is plotted in Figure 4. This boiling fraction is then used to evaluate the range of boiling heat transfer fractions during the initial blowdown for typical critical break and 100% RIH breaks in a CANDU reactor. The results are given in Figures 5 and 6. The upper and lower values shown in these figures correspond to a range of initial wall superheats on fuel sheaths in the high neutron importance region of the core that develop immediately following the initial coolant decompression of the coolant. The values of superheat are between 20 K and 25 K. These results demonstrate clearly the limitation on the boiling heat transfer due to rapidly nucleating and detaching vapour bubbles during the early stage of blowdown. This heat transfer limitation will also impose a limitation on the rate of coolant voiding due to coolant boiling heat transfer.

6. Conclusions

Analysis of the factors governing vapour nucleation, bubble detachment and transport has been performed using information available in the open literature. The analysis has been applied to the initial stages of blowdown in CANDU fuel channels following a LOCA to determine the potential limitation on boiling heat transfer from fuel elements due to finite times for transporting vapour away from the surface of fuel element sheaths.

The analysis demonstrates that in the first two seconds of blowdown boiling heat transfer will be limited to between approximately 60% to 80% of the fuel sheath area due to the accumulating vapor bubbles which are being transported away from the fuel sheath surface. These results are consistent with experimental observations obtained in blowdown tests performed in small-scale water and Freon test facilities.

The results of this analysis indicate that there are inherent limitations on boiling heat transfer from the higher power elements of fuel bundles in the high neutron importance regions of the core. Therefore, it can also be concluded that there are inherent limitations on the rate of coolant voiding due to boiling heat transfer and that this limitation is not dependent upon whether or not a fuel element experiences dryout. Further work is underway to extend this heat transfer model to transient coolant voiding and to validate the model against test data.

7. Acknowledgments

Financial support of the Natural Sciences and Engineering Council of Canada (NSERC) and the University Network of Excellence in Nuclear Engineering (UNENE) is gratefully acknowledged.

8. References

1. S.G. Bankoff, “Entrapment of Gas in the Spreading of a Liquid over a Rough Surface”, AICHE J., Vol. 4, p 24, 1958.
2. Y.Y. Hsu, “On the Size Range of Active Nucleation Cavities on a Heated Surface”, Trans. ASME, J. Heat Transfer, Vol. 98C, pp.207-216, 1962.
3. Y.Y. Han and P. Griffith, “The Mechanism of Heat Transfer in Nucleate Pool Boiling”, Int. J. Heat Mass Transfer, Vol. 8, pp 887-904, 1965.

4. B.B. Mikic and W.M. Rohsenow, "Bubble Growth Rates in Non-Uniform Temperature Field", Prog. Heat Mass Transfer, pp 283-293, 1969.
5. P. Griffiths and J.D. Wallis, " The Role of Surface Conditions in Nucleate Boiling", Chem. Eng. Progress Symp. Series, No. 30, Vol.56, pp. 49-63, 1960.
6. L.Z. Zeng and J.F. Klausner, "Nucleation Site Density in Forced Convection boiling", Trans. ASME, J. Heat Transfer, Vol. 115, pp.215-221, 1993.
7. N. Basu, G.R. Warrier and V.K. Dhir, "Onset of Nucleate Boiling and Active Nucleation Site density During Subcooled Flow Boiling", Trans. ASME, J. Heat Transfer, vol. 124, pp. 717-728, 2002.
8. C.H. Wang and V.K. Dhir, "Effect of Surface Wettability on Active Nucleation Site Density During Pooling of Water on a vertical Surface", Trans. ASME, J. Heat Transfer, vol. 115, pp. 659-669, 1993.
9. Hsu and Graham, "Transport Processes in Boiling and Two-Phase Systems", Hemisphere Publishing, Washington D.C., 1976
10. R.L. Judd, H. Merte and M.E. Ulucakli, "Variation of Superheat With Subcooling in Nucleate Pool Boiling", Trans. ASME, J. Heat Transfer, Vol. 113, pp. 201-208, 1991.
11. K. Fukuda, M. Shiotsu, K. Hata and A. Saurai, "Transient Boiling Heat Transfer from Initial Steady State Caused by Rapid Depressurization", Nuclear Engineering & Design, vol. 149, pp 97-110, 1994.
12. J.C.M. Leung, S.G. Bankoff, R.E. Henry and O.C. Jones, "Occurrence of Critical Heat Flux During Blowdown with Flow Reversal", Nuclear Engineering & Design, vol. 52, pp 303-324, 1979.

Table 1
Inferred Nucleation Site Density at Onset of Dryout
(Pressure = 9 Mpa, Quality = 5%)

Dryout Heat Fux [kW/m^2/^{o}C]	Mass Flow Rate at Dryout [kg/s]	Wall Superheat [^{o}C]	Nucleation Site Density [cm^{-2}]
1400	16	27.0	344.8
1000	10.6	27.6	380.7
800	8.13	27.9	399.6
550	5	27.5	374.5
200	1.45	27.9	399.6
146	1	28.0	406.1

Table 2
Typical Vapor Velocities, Characteristic Lengths and
Transport Times for Vapour Tranport

Component	Parameter	Characteristic Length [mm]	Characteristic Transport Time [s]
Boiling	*q=1400*	1.8 - 4.57	0.09 - 0.23
	q=800		0.15 - 0.38
	q=550		0.225 - 0.57
Bubble Rise		8.3 - 14.8	0.045 - 0.08
Vapour entrainment	*W=16*	250	0.038
	W=10		0.061
	W=5		0.123
	W=1		0.61
	W=0.5		1.25

q = heat flux in [kW/m^2]
W = Mass flow rate [kg/s]

Figure 1
Nucleation Site Density as a function of Wall Superheat and Coolant Pressure

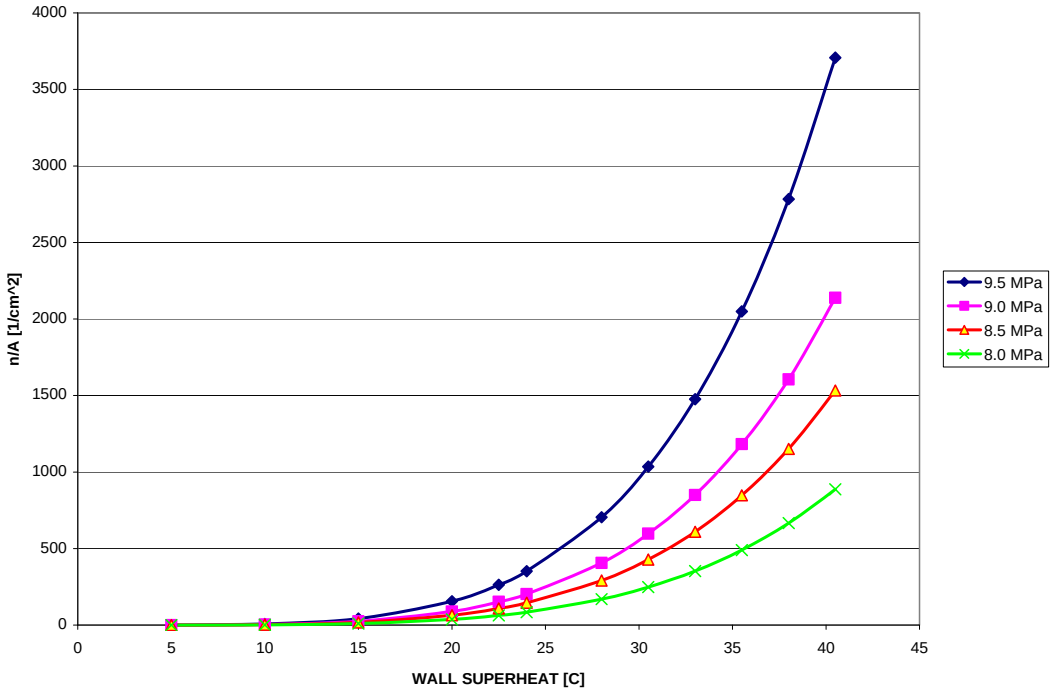

Figure 2
Characteristic Transport Times vs Coolant Mass Flow Rate

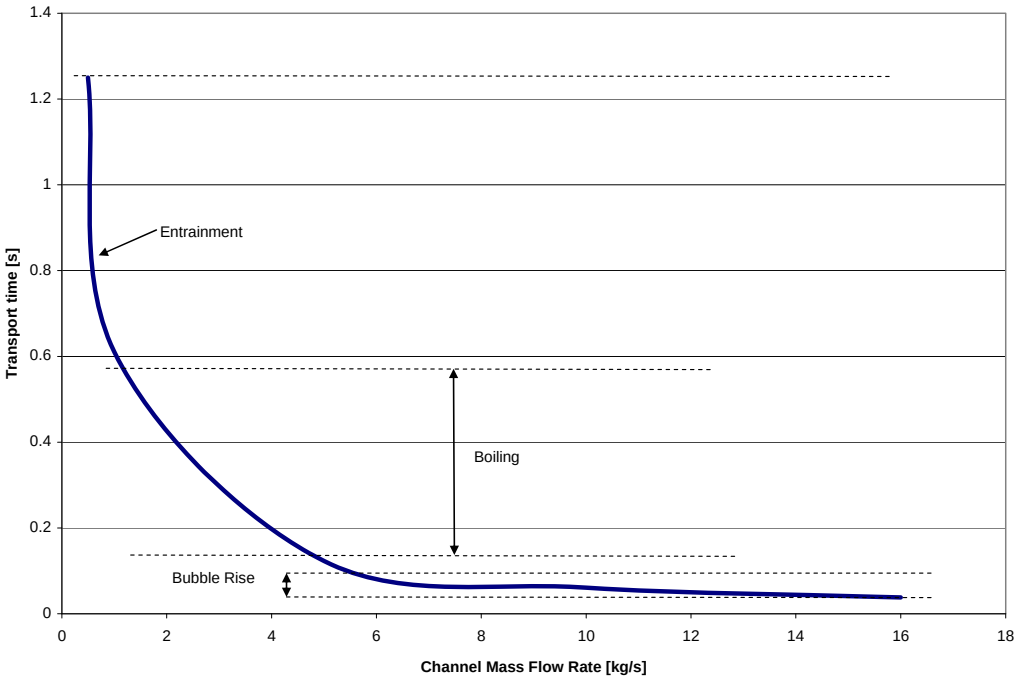

Figure 3
Variation of Wall Superheat and Nucleation Site Density in the early stages of a 100% RIH Break LOCA

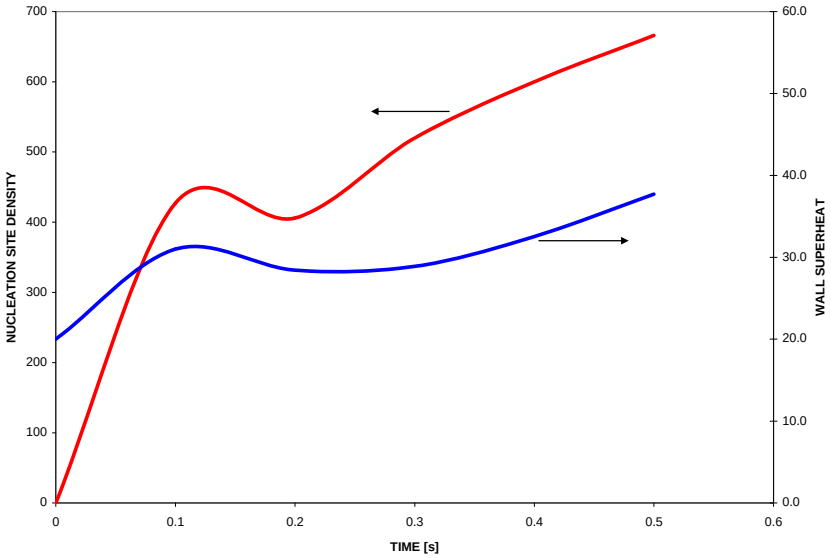

Figure 4
Fraction of Fuel Element Surface Area contributing to Boiling Heat Transfer as a function of Wall Superheat at various Coolant Pressures

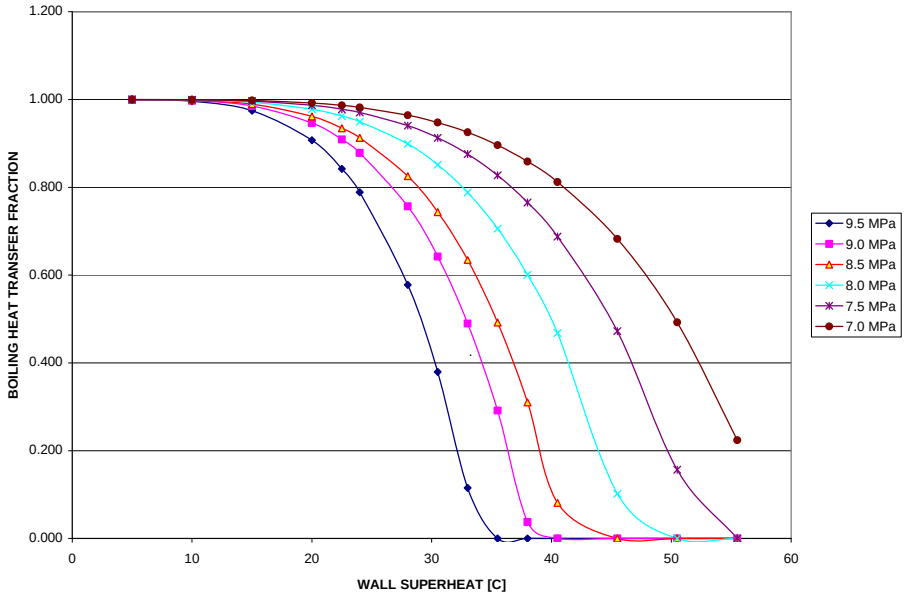

Figure 5
Fraction of Fuel Element Surface Area contributing to Boiling Heat Transfer
(100% RIH Break)

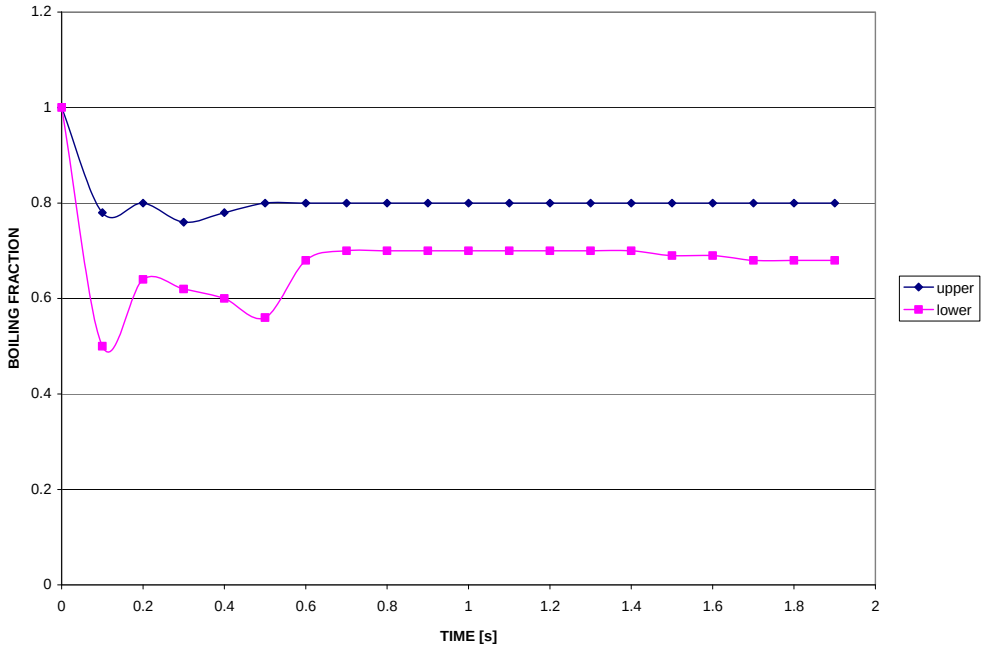

Figure 6
Fraction of Fuel Element Surface Area contributing to Boiling Heat Transfer
(Critical Break)